Zero : Jurnal Sains, Matematika, dan Terapan
E-ISSN : 2580-5754; P-ISSN : 2580-569X
Volume 9, Number 3, 2025
DOI: 10.30829/zero.v9i3.26871
Page: 970-979

Development of a Traffic Signal Green Time and Cycle Length Optimization Model Using NSGA-III

[1] **Meliana Pasaribu**
Department Mathematics, Universitas Tanjungpura, Pontianak, 78124, Indonesia

[2] **Helmi**
Department Mathematics, Universitas Tanjungpura, Pontianak, 78124, Indonesia

[3] **Adrah**
Department Mathematics, Universitas Tanjungpura, Pontianak, 78124, Indonesia

[4] **Eka Nisrina Yaqin**
Department Mathematics, Universitas Tanjungpura, Pontianak, 78124, Indonesia

Article Info

Article history:

Accepted, 26 December 2025

Keywords:

Capacity;
Delay;
Emissions;
Knee point.

ABSTRACT

Optimization of delay, capacity, and emissions in signalized intersections brings in conflicting goals. But most literature studies have dealt with these individual goals or used two-objective optimization methods, and such approaches are not efficient in capturing these tradeoffs. To overcome this problem, this research utilizes Non-dominated Sorting Genetic Algorithm-III in designing a model to optimize delay, capacity, and emissions for a four-leg intersection. Convergence, hypervolume indicator, and spread methods are used to examine algorithm performance, and knee point solutions are used to identify a tradeoff solution. The obtained output shows that NSGA-III gives a smooth and evenly spread Pareto front with a hypervolume 2.91×10^9 and a spread of 120.64, which represents excellent convergence and diversification capabilities. Following the outcome of the experiment based on knee point identification, the solution with index 38 gives an optimal control setting of q_1 = 37.7 s, q_2 = 20 s, q_3 = 20 s, q_4 = 27.8 s, with cycle length of C = 121.42 s. With this setting, the average delay is reduced by 38%, the queue length by 30%, and the degree of saturation is improved to 0.83, while capacity is reduced moderately and total emissions increased. In summary, this research work proves the NSGA III is efficient in identifying tradeoffs among delays, capacity and emission. The highlight of this research work is that the knee point gives the most balanced operational solution without excessively increasing cycle length.

Corresponding Author:

Meliana Pasaribu,
Department of Mathematics,
Universitas Tanjungpura, Pontianak, Indonesia
Email: meliana.pasaribu@math.untan.ac.id

1. INTRODUCTION

West Kalimantan is the fourth largest province in Indonesia, with an area of 140,307.00 km^2, representing about 7.53% of Indonesia's total area [1]. The region is also known as "Land of a Thousand Rivers" [2], therefore, it is necessary to provide bridges as a means of supporting the community's mobility. In the Kubu Raya region, the movement of traffic centers around a few major intersections, one of which is the Adisucipto-Major

Alianyang intersection. This intersection connects educational, commercial, and industrial areas, and serves as the primary access to the Kapuas II Bridge, the only bridge designed for heavy vehicles in the area.

Due to its strategic function and high traffic demand, congestion often occurs during peak hours at the Adisucipto- Major Alianyang intersections. Inadequate signal timing under such conditions results in excessive delays, long queues, increased fuel consumption, and higher exhaust emissions. Traffic in efficiency aside, these issues also carry serious environmental implications. The transport sector contributes approximately 29% of total energy consumption globally and contributes around 24% to global carbon dioxide emissions [3],[4]. On a local level, pollutant measurements on the Major Alianyang corridor reported CO concentrations reaching 53.33 $^{g}/_{m/h}$ [5] to an increase 9,537.12 $^{\mu g}/_{m^3}$ in 2019[6], because these are close to or over the critical levels of air quality. Emission quantities are worsened by frequent idling of the engine, repetition in acceleration, and driving at low speed, as typical conditions associated with signalized intersections in cases of congestion [3], [7], [8].

The Adisucipto–Major Alianyang intersection represents a complex traffic-signal control problem with mixed traffic conditiond and a considerable proportion of heavy vehicles. Such traffic conditions significantly influence saturation flow rates and delay formation, rendering the existing signal settings highly inappropriate. Optimization of signal timing is thus one of the critical interventions in this case, especially through multiobjective approaches that simultaneously consider both traffic efficiency and environmental performance. Previous studies have shown that multiobjective optimization frameworks outperform deterministic approaches to signal by achieving balanced improvements across multiple performance indicators. For example, models considering both delay and emission objectives have been shown to reduce waiting time and emissions more effectively than the traditional setting based on HCM 2010 [7]. Kwak ett al. reported that signal optimization in urban corridors can reduce fuel consumption by up to 20% and decrease emission by 8 – 20 %, along with improvement in travel time[9]. Furthermore, mult-objective evolutionary algorithm such as HCVSGA III have also been applied to jointly optimize delay, capacity, and emissions, achieving significant performance gains and emission reductions in several traffic scenarios [10].

With these advances, however, the signal timing optimization problem is still inherently complex: delay, capacity, and emissions are nonlinear and competing objectives, and no single solution can optimize all three simultaneously. These gives rise to a high dimensional, nonconvex solution space that is further constrained by minimum and maximum green time and cycle length bounds Such characteristics make traditional analytics or gradient-based optimization approaches inapplicable. Evolutionary algorithms are therefore befitting for such problems; NSGA-III is especially relevant since it works well for many objective optimization problems and handles solution diversity via reference directions. Despite a wide use of multiobjective evolutionary algorithms in international studies, the integration of green time and cycle length decision variables to deal with delay, capacity, and emission objectives via NSGA III remains limitedin the Indonesia context. This study gap is apparently significant for a signalized intersection with mixed traffic and dominated by heavy vehicles, such as Adisucipto-Mayor Alianyang, and thus calls for studies offering appropriate mathematical models that provide a quantitative analysis of the trade offs among competing objects. This research, therefore, proposes a multiobjective optimization model using green durations of each phase and the signal cycle length as decision variables. The developed model minimizes delay, maximizes capacity, and minimizes vehicle emissions simultaneously. NSGA is adopted to provide a representative Pareto-front under realistic timing constraints from which implementable and reasonably balanced signal timing solutions can be generated in order to improve the operational and environmental performance of the Adisucipto Major Alianyang intersection.

2. RESEARCH METHOD

The research methodology is designed to obtain optimal solutions for traffic signal timing at the Adisucipto–Major Alianyang intersection using a multi-objective optimization model based on the NSGA-III algorithm. The stages of research in this study include data collection, mathematical modeling, and computational optimization. Data used are of both primary and secondary sources, which contain information on each phase's traffic volume, geometric characteristics of the intersection represented by the number of lanes, lane width, and movement directions; existing signal characteristics expressed bycycle length, green–yellow–red split; vehicle composition represented by motorcycles, light vehicles, and heavy vehicles; and queue length and delay observations.

As the traffic composition at and approaching the intersection is heterogeneous and conflicting, all volumes in the intersection are normalized interms of passenger car units (PCU/smp) with recommended equivalency factors suitable for heterogeneous and conflicting traffic situations. Let V_i^k represent the observed volume corresponding to vehicle type k in phase i, and let α_k represent its PCU equivalency factor. Then equivalent traffic flow in phase i can be stated as

$$V_i = \sum_h \alpha_k V_i^k \tag{1}$$

Such a conversion will directly influence the optimization model. With respect to the delay function, V_i multiplies the total accumulated delay, which means a higher share of heavy vehicles will cause a higher share of

heavy vehicles will cause a higher level of system delay despite unchanged signal timings. On a parallel note, with regard toan emission function, PCU normalized flows will represent traffic demand with an effective consideration given to emission calculations in a unified unit system, despite different vehicle specifications. Therefore, variations in PCU composition directly alter the magnitude of both delay and emission objectives. This explains why phases dominated by heavy vehicles exhibit higher delay and emission values in the Pareto solutions, as discussed in Result and Analysis.

The traffic signal timing problem is modeled as a multi-objective optimization model with three conflicting objective functions namely minimization of delay, maximization of capacity, and minimization of vehicle emissions. The decision variables are the green times for each phase and the cycle length $x = (q_1, q_2, q_3, q_4, C)$. The total trafic delay is computed as

$$T(x) = \sum_{i=1}^{N} V_i T_i. \tag{2}$$

where T_i is the average delay per vehicle on phase i(seconds), and V_i is the number of vehicles on phase i, for $i = 1,2,3,4$. Traffic capacity is calculated using the proportion of green time:

$$D(x) = \sum_{j=1}^{m} \sum_{i=1}^{N} S_{ij} \lambda_i \,. \tag{3}$$

where S_{ij} is the saturation flow for phase $i$and entry lane j, and $\lambda_i = \frac{q_i}{C}$ is the green–to–cycle ratio for phase i. Since NSGA III is formulated as a minimization form, capacity is represented as:

$$f_2(x) = -D(x). \tag{4}$$

Total vehicle emissions are expressed as:

$$E(x) = \sum_{i=1}^{4} (EF \cdot q_i \cdot L_0 + \frac{1}{3600} \cdot EFI \cdot q_i \cdot T_i), \tag{5}$$

where EF is the emission factor under driving conditions (5 g/smp/km), q_i is the green interval (seconds), L_0 is the entry-lane length, and EFI is the emission factor under idling conditions (45 g/smp/km)[11]–[14].
The combined objective function is:

$$\min\ f(x) = (T(x),\ -D(x), E(x)). \tag{6}$$

The optimization problem is constrained by operating and feasibility considerations:

$$q_i{}^{min} \le q_i \le q_i{}^{max}, i = 1,2,3,4$$
$$C^{min} \le \mathrm{C} \le \mathrm{C}^{max}$$
$$C = \sum_i (q_i + l_i)$$

Where l_i denotes the lost time for phase i.

Operational feasibility is further ensured by enforcing the degree of saturation constraint $DS_i = \frac{v_i}{S_i \frac{q_i}{C}} \le 1, i = 1,2,3,4$. This condition guarantees stable traffic operation by preventing oversaturated phases and unbounded queue growth. Only solutions satisfying $DS < 1$ Are considered feasible and are retained for analysis, consistent with the selection of the knee point solution in the Result and Analysis.

The NSGA III algorithm is used because of its capability to form a Pareto front with good diversity with the aid of a reference point approach that boosts solution diversification [15], [16]. Althought the algorithm adheres to abroad evolution described in [16]–[18], being a part of an evolution strategy, a series of technique modifications are incorporated in consideration of heterogeneous traffic performance in signalized intersections. Initial populations are produced using random boundary initialization for green times and cycle length, explicitly considering boundary feasibility of signals to avoid an excessive generation of infeasible solutions right from

initialization phases. Unlike in common implementations of NSGA-III, where mainly dominance-based feasibility handling takes place, this work incorporates feasibility screening taking into consideration degree of saturation rules, among other rules in signal timing.

Every candidate solution is assessed with PCU flows in traffic, such that each objective, especially delay and emission takes into consideration the variability in heterogeneous traffic composition, which is implicitly considered in [16]–[18]. A non-dominated sorting and a selection using a reference point are used in this work, where, unlike [16], uniformly distributed directions are not used in this research, but directions are implicity indicated based on delays, capacity, and emission observed in a real intersection in a research study, hence generating a concentrated Pareto front.

The parameter settings of the algorithm are a balance between convergence speed and calculation efficiency. A population size of 100 is used to keep solution diversity without excessive computational cost [10], [19], [20]. A total of 200 generations is sufficient for a fixed point of stable convergence and is generally used in NSGA-III-based transportation studies[10], [20]. The number of decision variables is 5 (four green times and one cycle length). The crossover rate (PC = 0.9) provides intensive exploration in a continuous decision space. The mutation rate (PM= $= \frac{1}{N_{var}} = \frac{1}{5} = 0.2$) ensures, on average, one mutated variable per individual, consistent with evolutionary algorithm standards[21]–[23]. Distribution index $\eta_c = 20$ produces smooth offspring under simulated binary crossover, and $\eta_m = 20$ yields localized but stable mutations[23]. Lost times of 3, 5, 5, and 3 seconds are based on field observations of the signal phases.

Genetic operators operate in constraint-aware environments where children with inadmissible cycle length, minimum green time, or saturation are punished or fixed before selection. The evolution step ends when convergence is reached, which can be observed by the Pareto front becoming stable. The final solution takes the form of a Pareto-optimal solution, a Pareto front with tradeoffs in delay, capacity, and emissions. Pareto solutions are evaluated using two-dimensional and three-dimensional Pareto charts and contrasted with existing settings. A Pareto solution is finally identified based on knee point identification to be both mathematically optimal and feasible in terms of $DS < 1$ in practical traffic settings.

3. RESULT AND ANALYSIS

The Adisucipto–Mayor Alianyang intersection is a four-leg signalized junction operating with four traffic signal phases. Vehicle movements at the intersection consist of four phases. Vehicle movements at the intersection consist of four phases, as shown in Figure 1, each representing movements from the four approaches of the junction.

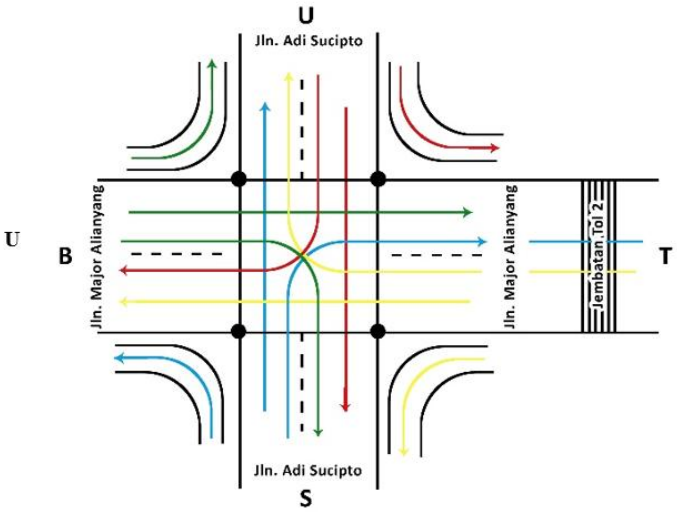

Figure 1. Traffic Signal Phases at the Major Alianyang-Adisucipto Intersection

Each phase corresponds to movements coming from a certain approach. Phase 1 (Red) allows movements from Adisucipto Road (West) to the other three directions. Phase 2 (Yellow) allows movements from Mayor Alianyang (North). Phase 3 (Green) allows movements from Mayor Alianyang (South). Phase 4 (Blue) allows movements from Adisucipto (East). Traffic volume data for vehicles passing through the Adisucipto–Mayor Alianyang intersection on 5 October 2021 between 16:00–17:00 WIB were obtained from field observations and are presented in Table 1.

Table 1. Traffic Volume at the Adisucipto – Mayor Alianyang intersection (16:00 – 17.00)

Vertex	Motorcycles	Light Vehicles	Heavy Vehicles
1	2.873	394	233
2	2.487	267	183
3	2.176	235	147
4	2.673	479	267

The stream traffic behavior at the intersection of Adisucipto-Major Alianyang Street is affected by conflicting traffic situations with overlapping green time phases, which form interweaving paths among vehicles [24], [25]. Due to varying dimensions and traffic dynamics of motorcycles, light vehicles and heavy vehicles, all volume measurements will be normalized using passenger car units (pcu/h) in accordance with recommended equivalency factors under conflicting traffic [26]–[28]. The PCU conversion in this research work adopts the Indonesian Highway Capacity Manual (MKJI) standard, considering the equivalence factor of 0.4 for motorcycles, 1.0 for light vehicles, and 1.4 for heavy vehicles, based on their space occupancy and maneuvering capabilities in traffic flow. Normalization of traffic volume is conducted through Equation (1) below, which signifies a weighted combination of various vehicle types to approximate an effective rate of flow for each phase of a signal. A higher PCU weight is given to heavy vehicles because of their size and capacity restrictions, and a lower weight is given to motorcycles because of their smaller size and higher maneuverability. Such PCU standardization helps in a unified treatment of diversified traffic demand in calculations pertaining to delay, capacity, emissions, and degree of saturation, ensuring the viability of solutions under Pareto optimality highlighted in 'Results and Analysis'. The resulting total traffic volume and losses in each phase are given in Table 2 below.

Table 2. Total Traffic Flow and Lost time for Each Phase

Vertex	Total Traffic Flow ($Q(x)$)	Lost time (second)
1	1911	3
2	1499	5
3	1296	5
4	1895	3

Traffic characteristics indicate the imbalance of high flow phases, Phase 1 and Phase 4 versus flow flow phases, Phase 2 and Phase 3. Such an imbalance may increase delay and queue length, making optimized signal timing highly essential. Formulating the problem into an optimization model [29]
The decision variables are the green times for each of the four phases and the cycle length:

$$x = (q_1, q_2, q_3, q_4, C).$$

Three objective functions are optimized simultaneously
Minimization of Traffic Delay:

$$T(x) = \sum_{i=1}^{4} V_i T_i$$

Maximization of intersection capacity:

$$D(x) = \sum_{j=1}^{4} \sum_{i=1}^{4} S_{ij} \lambda_i.$$

Minimization of Exhaust emissions:

$$E(x) = \sum_{j=1}^{4} \left(EF \times q_i \times L_0 + \frac{1}{3600} \times EFI \times q_i \times T_i \right)$$

Since NSGA-III is formulated for minimization[30], the capacity objective is expressed as $-D(x)$. Thus, the multi-objective optimization model is expressed as

$$f(x) = \min(T(x), -D(x), E(x)).$$

Cycle Length Constraint

$$90 \leq C \leq 180\,.$$

Minimum Green Time constraint

$$q_i > 20\,;\mathrm{i} = 1,2,3,4.$$

Signal Cycle Structure

$$C = \sum_i (q_i + l_i).$$

Optimization by NSGA-III generates a set of nondominated solutions that forms the Pareto Front. Each solution represents one combination of green times (q_1, q_2, q_3, q_4) and cycle length C, that corresponds to a different trade off among three objectives. The numerical scale in the Pareto graphics is as follows total delay $28{,}000 - 38{,}600$ seconds, emission $125 - 129$ units and capacity $1530 - 1533\,pcu/h$. These narrow ranges indicate that even small changes in signal timing produce strong interactions among the objectives. To clarify the relationship between objectives between delay and capacity, delay and emissions, capacity and emissions, the following is given in Figure 2.

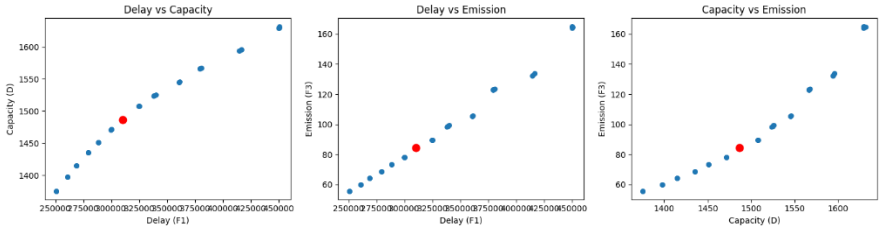

Figure 2. Pareto Front Relationships: (a) Delay – Capacity, (b) Delay – Emission, (c) Capacity - Emission

Visualization in Figure 2(a) shows a positive (monotonic increasing) relationship between delay and capacity. Capacity increases can only be achieved by extending green time. However, this extension also increases cycle length, increasing the accumulated delay. Thus, there is a direct conflict between T(x) and D(x). Figure 2.b. shows a nearly linear relationship, with greater delays resulting in greater emissions. This is because vehicles waiting for long periods of time in idle conditions increase fuel consumption and emissions. Figure 2.c. shows that increased capacity results in an increase in the number of vehicles served. Thus, total engine activity increases, resulting in increased total emissions from vehicles.

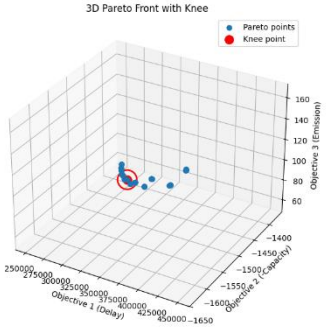

Figure 3. The distribution of Pareto-optimal solutions in the three-objective space

The 3D Pareto Front visualization can be seen in Figure 3, which provides a comprehensive overview of the conflict between the three objectives. The resulting Pareto surface is concave, indicating dominance by several central solutions offering the best compromise. From the distribution pattern, one point with a significant change in curvature is visible, namely the knee point[31], a solution that provides an optimal balance between delay, capacity, and emissions.

The detected knee point corresponds to $q_1 = 37.7\,s, q_2 = 20\,s, q_3 = 20\,s, q_4 = 27.8\,s$ and $, C = 121.42\,s$.

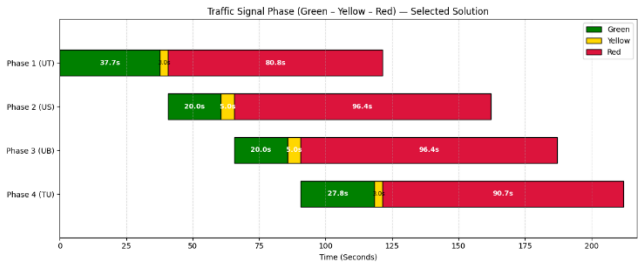

Figure 4. Signal Phase Diagram

Phases 1 and 4 are assigned longer green intervals, reflecting their higher traffic demand. Minimum operational green times, however, are still assigned for phases 2 and 3. The 121.42-second cycle length provides stable operation without excessive delay increases.

In Figure 4, the phase diagram represents the entire structure of the signal, which forms the direct basis of the input for generating those points in the Pareto graph-delay, capacity, and emissions. Figure 3: The 3D Pareto front represents the complete picture of the trade-offs among the three objective functions; it shows the shape of the front, its curvature, and where the knee point lies. Meanwhile, Figure 2 presents a projection of the relationships of two objectives for the sake of clarity of visual interpretation. All numerical values across the three visualizations have their root in the same decision variables; they are simply visualized in a different way. The three figures are interconnected: 3D Pareto front displays positions of the solution within the conflict space, the 2D Pareto charts explain the relationship between objectives, and the phase diagram explains what system mechanism yields those values.

Theherefore, the quality of the Pareto solution is evaluated by four indicators. First is the convergence performance. A smooth Pareto front without outliers shows that the convergence is close to the global optimum. Solution coverage quality relative to the reference point is measured by the Hypervolume value [32]. A hypervolume value of 2.914538×10^9 shows that the solution coverage is wide, with excellent solution exploration quality. The Spread value is 120.642, which means an even distribution of pronts and no overlapping solutions. The summary of the traffic performance parameters before and after the optimization can be seen in Table 3.

Table 3. Performance Comparison Before and After Optimization

Indicator	Before Optimization	After Optimization (Knee Point)	Change
Total Capacity ($\frac{pcu}{h}$)	6601	6132	-7.1%
Average Delay(s/veh)	61.55	38.1	-38%
Queue Length (m)	32.97	23	-30%
Degree of Saturation (DS)	1.09	0.83	$DS < 1$ (improved)
Emission	53.3 [5]	84.509	Increased
Cycle Length (s)	-	121.4	

Table 3 shows that emissions increased, while delays and queues were significantly lower. The increased capacity meant more vehicles were on the move, resulting in increased total emissions. To develop a deeper understanding of the interacting relationship between the objectives, a sensitivity analysis was performed. The average results can be seen in Table 4.

Table 4. Sensitivity Of Inter-Objective Relationships

Change	Average Impact
Delay decreased by 10%	Capacity decreased by 3.5%, Emissions decreased by 6.8%
Capacity increased by 10%	Emissions increased by 8.1%, Delays increased by 12.4%
Emissions decreased by 10%	Delays decreased by 8.7%, Capacity decreased by 5.3%

Table 4 reveals that with decreased delays, both capacity and emissions are reduced. The interpretation of this observation is that smoothing of flow tends to decrease queue and idle time but decreases the maximum capacity that can be passed in a single cycle. Moreover, when capacity increases, emissions increase along with delays. This is due to the fact that increasing the capacity in one arm is often at the expense of the other arm, and then asymmetric queues are developed. When emissions are reduced, both delay and capacity decrease. The

implication of this observation is that an environmentally friendly signaling scheme tends to be conservative with smoother phase changes to reduce the maximum capacity.

Results show that the three objectives conflict strongly and nonlinear. The complexity has been well captured by NSGA-III to provide a stable and well-distributed Pareto set. Not only has it converged toward an optimal solution, but also diversity has been preserved for decision-makers who evaluate various operational scenarios. Among all solutions, the knee point offers the most practical balance; substantial reductions in delay and queue length are achieved, while capacity and operational stability remain acceptable $DS < 1$. Though it does not minimize emissions, it represents the most implementable setting for real-world traffic control. The result is an assurance that multi-objective optimization gives a much closer approximation to the real-world intersection behavior than single-objective optimization does, especially in systems with interactions among competing performance criteria.

4. CONCLUSION

This article presents a multi-objective optimization model for signal control at the Adisucipto–Mayor Alianyang intersection, considering three objectives: delay minimization, maximization of capacity, and exhaust emissions minimization, using the NSGA-III algorithm. Aside from discussing the quantitative results, the significance of the proposed methodological contribution lies in the combined formulation process for different traffic flows, including PCU normalization, degree of saturation function constrains ($DS < 1$), and decision selections involving the knee points in the NSGA-III algorithm.These tasks make it possible to maintain the diversity of solutions while at the same time ensuring the feasibility of the solution for optimizing objectives involving efficiencies and environment.

The results show that NSGA-III has an evenly spread Pareto front that captures all trade-offs between objectives. The analysis of Pareto fronts in 2D and 3D diagrams shows similar quantitative characteristics. There is an exact trade-off between delay and capacity, and when delay is decreased by 10%, capacity decreases by 3.5% approximately. There is an exact monotonic increase between capacity and emissions, and when capacity is increased by 10%, emissions increase by 8.1% approximately, proving that with an increase in capacity, more vehicles are being processed, and effective green time is longer, thus influencing overall engine activity. There is an almost linear trade-off between delay and emissions, and when emissions are reduced by 10%, delay is reduced by 8.7% approximately, proving that in the signal phase, green time has an equal effect on delay, capacity and emission. The representative solution obtained using knee point identification results in $x = (37.7, 20, 20, 27.8)$ seconds and a cycle length $C = 121.4$ second. Compared to the previous conditions, the average delay reduces by 38% (61.55 seconds to 38.1 seconds) with the queue reduced by 30%, and the level of saturation increases to 0.83 encuring stability. Capacity reduces slightly by 7.1%, and the level of saturation increases to 0.83, ensuring stability. Capacity reduces slightly by 7.1%, and the emission amounts increase to 84.5 currently at 53.3, reflecting the increased number of vehicles and the smoothness of the traffic stream. Performance analysis results provide the hypervolume value to be 2.914538 x 10^9, and the spread measure recorded 120.64, identifying efficient convergence and diversification. Conclusively, the use of NSGA III proves to be effective in decoding multi-dimensional trade offs, providing adaptive and feasible signal timings. Its drawbacks are the absence of dynamic traffic, uniform vehicle movement, and the lack of turning movement and the priority vehicles. The focus of the subsequent investigation might revolve around using real-time detectors and CCTV information, focusing on short interval traffic, and employing adaptive and priority concepts for controlling signals.

5. REFERENCES

[1] Y. Ilham, E. Saputra, R. Wahid, and S. Insani, "Model WebGIS Menggunakan Metode Scoring Untuk Klasifikasi Tingkat Rawan Kebakaran Hutan di Kalimantan Barat," *Progresif J. Ilm. Komput.*, vol. 20, no. 1, pp. 403–416, 2024, [Online]. Available: https://doi.org/ 10.35889/progresif.v20i1.1692

[2] N. Sa'adah, P. Subardjo, W. Atmodjo, and M. F. A. Ismail, "Laju Sedimen Menggunakan Metode Isotop 210pb Di Muara Jungkat Pontianak Kalimantan Barat.," *J. Oceanogr.*, vol. 4, no. 1, pp. 48–54, 2015.

[3] Z. M. Chen and G. Q. Chen, "Embodied carbon dioxide emission at supra-national scale : A coalition analysis for G7 , BRIC , and the rest of the world," *Energy Policy*, vol. 39, no. 5, pp. 2899–2909, 2011, doi: 10.1016/j.enpol.2011.02.068.

[4] G. Q. Chen, X. D. Wu, J. Guo, J. Meng, and C. Li, "Global overview for energy use of the world economy : Household-consumption-based accounting based on the world input-output database (WIOD)," *Energy Econ. J.*, vol. 81, no. 81, pp. 835–847, 2019, doi: 10.1016/j.eneco.2019.05.019.

[5] Winardi, "Dispersi Gas Karbon Monoksida (CO) Dari Sumber Transportasi Di Kota Pontianak," *SEMIRATA 2015*, pp. 737–746, 2015.

[6] R. Andriani, R. Adriat, and J. Gajah, "Konsentrasi Karbon Monoksida (CO) di Kota Pontianak," *Prism. Fis.*, vol. 7, no. 2, pp. 143–148, 2019.

[7] W. Kou, X. Chen, L. Yu, and H. Gong, "Multiobjective optimization model of intersection signal timing considering emissions based on field data : A case study of Beijing," *J. Air Waste Manage. Assoc.*, vol. 68, no. 8, pp. 836–848, 2018, doi: 10.1080/10962247.2018.1454355.

[8] T. J. Wallington, J. E. Anderson, R. H. Dolan, and S. L. Winkler, "Vehicle Emissions and Urban Air Quality : 60 Years of Progress," *Atmosphere (Basel).*, vol. 13, no. 5, p. 650, 2022, [Online]. Available: https://doi.org/10.31004/innovative.v4i4.13761

[9] J. Kwak, B. Park, and J. Lee, "Evaluating the impacts of urban corridor traffic signal optimization on vehicle emissions and fuel consumption," *Transp. Plan. Technol.*, vol. 35, no. October 2014, pp. 145–160, 2012, doi: 10.1080/03081060.2011.651877.

[10] X. Zhang *et al.*, "Intersection Signal Timing Optimization : A Multi-Objective Evolutionary Algorithm," *Sustainability*, vol. 14, no. 3, pp. 1–16, 2022, [Online]. Available: https://doi.org/10.3390/su14031506

[11] K. L. Hidup, *Pedoman teknis penyusunan inventarisasi emisi pencemar udara di perkotaan*. Jakarta: Kementrian Lingkungan Hidup, 2013.

[12] D. A. Dewanto, B. Y., Dirgawati, M., Permadi, "Inventarisasi Emisi Pencemar Kriteria dan Gas Rumah Kaca dari Sektor Transportasi On- Road di Kota Bandung menggunakan Model International Vehicle Emissions (IVE)," *J. Reka Lingkung.*, vol. 9, no. 2, pp. 132–144, 2021, [Online]. Available: https://doi.org/10.26760/rekalingkungan.v9i2.132-144

[13] R. S. Abdullah, "Integrated Corridor Management Operation Strategies," Istanbul Technical University, 2017.

[14] G. Hadi, M., Tariq, M. T., Saha, R. C., Wang, T., & Pacal, "Comparing & Combining Existing & Emerging Data Collection & Modeling Strategies in Support of Signal Control Optimization & Management," 2021.

[15] K. Deb and H. Jain, "An Evolutionary Many-Objective Optimization Algorithm Using Reference-Point-Based Nondominated Sorting Approach , Part I : Solving Problems With Box Constraints," *IEEE Trans. Evol. Comput.*, vol. 18, no. 4, pp. 577–601, 2014, doi: 10.1109/TEVC.2013.2281535.

[16] R. H. Bhesdadiya, I. N. Trivedi, P. Jangir, and N. Jangir, "An NSGA-III algorithm for solving multi-objective economic / environmental dispatch problem," *Cogent Eng.*, vol. 47, no. 1, 2016, doi: 10.1080/23311916.2016.1269383.

[17] J. B. B, K. Deb, and P. C. Roy, *Investigating the Normalization Procedure of NSGA-III*. Springer International Publishing, 2019. doi: 10.1007/978-3-030-12598-1.

[18] Z. Cui, Y. Chang, J. Zhang, X. Cai, and W. Zhang, "Improved NSGA-III with selection-and-elimination operator," *Swarm Evol. Comput.*, vol. 49, no. May, pp. 23–33, 2019, doi: 10.1016/j.swevo.2019.05.011.

[19] Y. Song, R., He, S., & Yang, "Combined Genetic Algorithms for Solving the Location Problem of Public Transit Rescuing Centers* Rui Song 1, Shiwei He 2, Yongkai Yang 3," *Traffic Transp. Stud.*, vol. 959–964, no. 79800001, pp. 959–964, 2002, [Online]. Available: https://doi.org/10.1061/40630(255)134

[20] T. S. Vermeulen, "A Framework for Medium-Fidelity Ducted Fan Design Optimisation," Delft University of Technology, 2025.

[21] A. Hassanat, K. Almohammadi, E. Alkafaween, and E. Abunawas, "Choosing Mutation and Crossover Ratios for Genetic Algorithms — A Review with a New Dynamic Approach," *Information*, vol. 10, no. 12, p. 390, 2019, doi: 10.3390/info10120390.

[22] H. Seada and K. Deb, "U-NSGA-III : A Unified Evolutionary Algorithm for Single , Multiple , and Many-Objective Optimization," 2014.

[23] A. M. Abdelkhalek, A. Mohammed, M. A. Attia, and N. Badra, "An Enhanced Genetic Algorithm Using Directional-Based Crossover and Normal Mutation for Global Optimization Problems," *Stat. Optim. Inf. Comput.*, vol. 12, no. March, pp. 446–462, 2024, doi: 10.19139/soic-2310-5070-1796.

[24] R. Nasmirayanti, "Perencanaan Ulang Pengaturan Fade Alat Pengatur Lalu Lintas Pada Persimpangan Bersinyal Di Persimpangan Jl. Jendral Sudirman – KIS Mangun Sarkono," *Rang Tek. J.*, vol. 2, no. 1, pp. 132–143, 2019, [Online]. Available: https://doi.org/10.31869/rtj.v2i1.775

[25] Indah, R. Tumilaar, and C. E. J. C. Montolalu, "Optimasi Pengaturan Lampu Lalu Lintas dengan menggunakan Metode," *d ' Cartes. J. Mat. dan Apl.*, vol. 8, no. 1, pp. 27–35, 2019, [Online]. Available: https://doi.org/10.35799/dc.8.1.2019.24590

[26] G. R. Prima, H. Iskandar, and T. B. Joewono, "Kajian Nilai Ekivalensi MMobil Penumpang Berdasarkan Data Waktu Antara Ruas Jalan Tol (A Study Of Passenger Car Equivalency Based On Headway For Toll Roads)," *J. Jalan Jemb.*, vol. 31, no. 2, pp. 74–82, 2018, [Online]. Available: https://binamarga.pu.go.id/jurnal/index.php/jurnaljalanjembatan/article/view/146

[27] T. D. Rosadi, "Penggunaan Okupansi dan Komposisi Kendaraan untuk Menentukan Ekivalensi Mobil Penumpang (EMP) Pada Lalu Lintas Campuran di Bundaran Empat Lengan," *Teras J. J. Tek. Sipil*, vol. 9, no. 2, pp. 125–132, 2019.

[28] M. E. Rachmanudin, W. A. Hermawan, and V. N. Saputra, "Upaya Mengetahui Nilai Derajat Kejenuhan Pada Jam Puncak Di Simpang Tiga Lengan Tak Bersinyal Jalan Kertawibawa – Jalan Syekh Maqdum Wali Purwokerto," *Innov. J. Soc. Sci. Res.*, vol. 4, no. 4, pp. 6973–6988, 2024.

[29] M. Pasaribu, Meliana; Kiftiah, *Pemrograman Linier: Seri Metode Grafik dan Metode Simpleks*. Untan Press, 2024.

[30] X. Xu, D. Cheng, D. Wang, and Q. Li, "An Improved NSGA-III with a Comprehensive Adaptive Penalty Scheme for Many-Objective Optimization," *Symmetry (Basel).*, vol. 16, no. 10, pp. 1–18, 2024, doi: https://doi.org/10.3390/sym16101289.

[31] G. Yu, L. Ma, Y. Jin, W. Du, Q. Liu, and H. Zhang, "A Survey on Knee-oriented Multi-objective Evolutionary Optimization," *IEEE Trans. Evol. Comput.*, vol. 26, no. 6, pp. 1–21, 2022, doi: 10.1109/TEVC.2022.3144880.

[32] A. P. Guerreiro and C. M. Fonseca, "The Hypervolume Indicator : Computational Problems," vol. 54, no. 6, 2021, doi: 10.1145/3453474.